IEEE Access
Multidisciplinary | Rapid Review | Open Access Journal

Received August 15, 2019, accepted September 9, 2019, date of publication September 20, 2019, date of current version October 2, 2019.

Digital Object Identifier 10.1109/ACCESS.2019.2942689

Selective Magnetic Abrasive Finishing of Nano-Thickness IZO-Coated Pyrex Glass Using Acoustic Emission Monitoring and Artificial Neural Network

JUNGSUN KIM[1], HYOJEONG KIM[2], AND SEOUNG HWAN LEE[3]

[1]Department of Computer Science and Engineering, Hanyang University, Ansan 15588, South Korea
[2]Graduate School, Department of Mechanical Design Engineering, Hanyang University, Seoul 04763, South Korea
[3]Department of Mechanical Engineering, Hanyang University, Ansan 15588, South Korea

Corresponding author: Seoung Hwan Lee (sunglee@hanyang.ac.kr)

This work was supported in part by the Basic Science Research Program through the National Research Foundation of Korea (NRF) under Grant NRF-2017R1D1A1B03035551.

ABSTRACT In this study, a novel setup for a nanoscale finishing process - magnetic abrasive finishing (MAF) - was investigated together with in-process monitoring using acoustic emissions (AE). A specially fabricated direction control piece with a neodymium magnet was attached to an MAF setup to perform surface finishing of thin-film (IZO) coated Pyrex glass workpieces within a selective area. For the selective finishing experiments, design of experiment (DOE) was applied to optimize the surface roughness of the workpieces. In addition, an acoustic emission (AE) sensor, which can effectively monitor surface roughness and process states during ultraprecision machining/polishing of nanoscale workpieces, was adopted to detect the depth of the polished surface during MAF. The experimental results show that the proposed MAF setup produces uniform surfaces with nano-level surface roughness in a confined (target) area. Moreover, AE monitoring appears to have strong correlations with process states and sufficient sensitivity to detect the critical thickness (the end point of the coating layer). The processed AE signals were utilized as input parameters for an artificial neural network (ANN) to determine whether the polishing was reached to the coating-substrate (Pyrex) boundary. With the proposed polishing and monitoring scheme, controlled nano-finishing of a thin film coated material are feasible in a selective area within specific thickness/layer.

INDEX TERMS Acoustic emission monitoring, artificial neural network, coating-substrate boundary, magnetic abrasive finishing, selective nano finishing, surface roughness.

I. INTRODUCTION

With the advent of nanotechnology, the possibility of using nanoscale thin films in electronics/medical applications and MEMS/NEMS (micro/nano electromechanical systems) has increased rapidly [1]–[3].

For example, a transparent conductive coating (zinc-doped indium oxide (IZO)) on Pyrex glass can be utilized for next-generation flexible displays and ultra-precision electronic devices [4], [5]. More often than not, such devices are fabricated by applying appropriate modification/patterning technologies to nanoscale thin films within a confined area [6]. Therefore, they require a selective nanoscale precision finishing technology, such as MAF (magnetic abrasive finishing), that provides process area and thickness control capabilities [7]. MAF is an efficient surface finishing technique that uses abrasive particles as flexible polishing tools in a magnetic field near the working area [8]. This process can achieve nanometer-range surface roughness on various surfaces, such as optical (aspherical) components and ultra-precision laser components. In addition, it can be used to eliminate defects for the passivation of interfaces in electronic and photovoltaic devices. In general, MAF minimizes the occurrence of micro cracks on the surface of brittle workpieces by using so-called magnetic abrasive brush, which generates very low and controllable forces [9]. For that

The associate editor coordinating the review of this manuscript and approving it for publication was Mostafa Rahimi Azghadi.

reason, it can be particularly useful in enhancing the surface quality of hard coating materials (Ra value in the nanometer range) such as IZO and thin oxide films.

To implement MAF, clarifying the relationship between the final surface texture and major process parameters (such as rpm, abrasive particle size, and gap) has been the main research focus for both theoretical/simulation and experimental studies [9]–[11]. In this research, a specially designed MAF setup was realized to perform ultraprecision surface finishing of a controlled area of nano-thickness (less than 200nm) IZO-coated Pyrex glasses. The polishing specimens (IZO films on Pyrex glasses) were prepared using radio frequency (RF) sputtering, which are frequently used for various materials, including non-metals, dielectric materials, and oxides. For the selective finishing experiments, design of experiment (DOE) was applied to select and evaluate the process parameters that dictate the surface roughness of the workpieces. In addition, an acoustic emission (AE) sensor, which can effectively monitor surface roughness and process states during ultraprecision machining/polishing of nanoscale workpieces [12], [13], was adopted to detect the depth of the polished surface during MAF. Based on the AE signals from the monitoring experiments, relevant features of the surface characteristics were extracted, and the feature vectors were used to construct an artificial neural network (ANN) as a critical layer (coating-substrate boundary) detection tool.

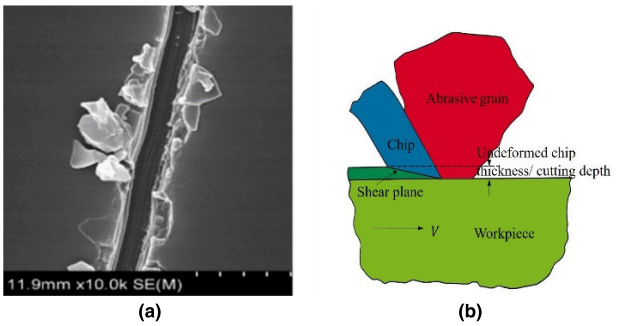

FIGURE 1. Brittle fracture (cracks) on the IZO-coated Pyrex glass and a ductile fracture (chip making) by an abrasive particle. (a) Brittle fracture (cracks) on the IZO-coated Pyrex glass after AFM nano machining (tip nose radius = 100nm), (b) Schematic of ductile mode cutting by an abrasive particle (applicable to Pyrex glasses).

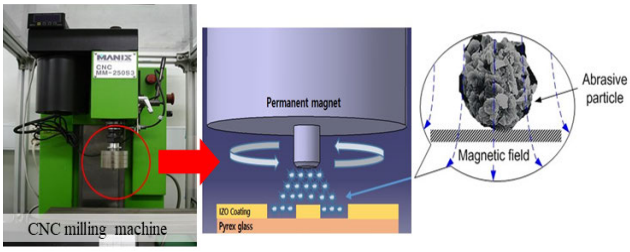

FIGURE 2. Schematic of the magnetic abrasive finishing of the coated Pyrex glass. Bonded abrasive particles (diamond + iron) were used for the process.

II. THEORETICAL BACKGROUND

A. IZO-COATED PYREX GLASS AND MAF

Pyrex glass, a special purpose glass, is frequently used in reflective optics for semiconductor parts and in bio-applications due to its chemical stability, low thermal expansion, and heat shock resistance. IZO thin films, which have many favorable properties such as transparency, high conductivity, and structural stability, have been used in various optical/electronic devices, including diodes, thin film transistors, next-generation flexible display electrodes, and solar cells [5], [6]. A transparent, conductive hard coating (IZO coating) on softer Pyrex glass can not only protect the substrate, but also take advantages of desirable property combinations from both materials.

Polishing a thin hard coating on a soft substrate produces distinct fracture behaviors [14], [15]. Generally, brittle materials (e.g., IZO) show brittle fractures (cracks), and ductile materials (Pyrex glass) go through plastic flow (Fig. 1). Therefore, if the polishing process reaches the substrate boundary, the basic material removal mechanism changes, which can be a major source mechanism for AE monitoring.

Fig. 2 presents a schematic of MAF and an image of the bonded abrasive particles used in this research. In MAF, abrasive particles are used as flexible finishing tools with surrounding magnets that generate a magnetic field around the polishing area. This research used a permanent magnet mounted on the spindle of a CNC machine (MM-250S3), which provides the following advantages: a magnetic pole with permanent magnetism, strong magnetic field intensity, low energy and cost, small size and light weight, and high revolutions with an easy tool change [8].

A bonded abrasive method [16] was adopted to combine the abrasive and magnetic particles. Compared to existing bonding methods, including sintering, the bonded abrasive method has advantages such as preventing magnetic weakening and providing simple bonding processes [17]. The magnetic (iron carbonyl) and abrasive (diamond) particles, which are used as flexible finishing tools, were mixed (mixing ratio 6:4) and combined using a cyanoacrylate-based binder. The sizes of the magnetic abrasives ranged from 25 to 75 μm, with an average value of 50 μm.

The Preston equation [18] is frequently used to interpret mechanical removal in loose abrasive processes. The Preston model describes the volumetric removal rate at point P on a workpiece as proportional to the normal load and the relative velocity:

$$\frac{\Delta h}{\Delta t}|_P = C\frac{\Delta L}{\Delta A}\frac{\Delta s}{\Delta t}|_P \tag{1}$$

Here, h is the depth of wear, A is the contact area, L is the total normal load, s is the sliding distance, and t is the processing time. C is a proportionality constant (Preston's coefficient) that depends on the quill condition, abrasive particle properties, slurry, and material properties of the workpiece.

Although the Preston model is widely used as a basic model, Bulsara *et al.* [19] suggested a more descriptive form

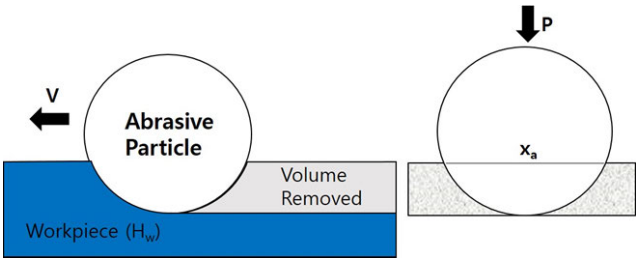

FIGURE 3. Schematic of the material removal action by a single abrasive particle.

of the Preston model to depict the polishing action of an abrasive particle (Fig. 3). The mean volume removed ($V_{removed}$) by a single abrasive per unit time can be expressed as

$$V_{removed} = C_1 x_a^2 (P^{1/3}/H_w)^{3/2} V \tag{2}$$

Here, C_1 is a proportionality constant that depends on the properties of the abrasive particles and slurry, as well as the material properties of the workpiece, x_a is the average size of the abrasives, P is the pressure, H_w is the workpiece hardness, and V is the relative velocity during polishing. Among the performance indices of polishing processes including MAF, the surface roughness is a key factor which reflects the stability and the efficiency of the process, along with material removal rate (MRR) [7], [10]. By selecting appropriate process variables based on process characterization, high quality surface finishing can be achieved and the controllability of the process will be significantly improved subsequently.

B. AE SIGNALS DURING MAF

AE is the low-intensity transient elastic waves generated by the rapid release of strain energy from localized source(s) within a material. These high-frequency (100 kHz to 1 MHz) waves propagate in all directions through the inside structure to a (piezo) transducer on the surface of the workpiece. Previous research has shown that AE is sensitive to a variety of characteristics in precision manufacturing processes, such as AFM nano machining, micro indentation/ scratching, and ultraprecision metal cutting [20]–[22]. The generation of AE signals is most influenced by the attributes of the materials being processed, and relevant information can be extracted from AE signals using various signal processing techniques, including time series and spectral analyses. Processed AE signals usually provide rich information about polishing states in real-time for process monitoring.

The AE energy (AE_{rms}, $\overline{AE}$) released is proportional to the plastic work rate ($\dot{W}$) absorbed by the material [23]

$$\left[\overline{AE}\right]^2 \propto \dot{W} \tag{3}$$

Also, the work rate of plastic work over the volume (V_w) of material under deformation is given by [24] as

$$\dot{W} = \sigma \cdot \dot{\varepsilon} \cdot V_w \tag{4}$$

where σ is the effective stress and $\dot{\varepsilon}$ is the effective strain rate.

In addition, AE energy is linearly proportional to the work rate [25] and eventually to the removal rate of the plastically deformed volume (material removal rate (MRR)) during the polishing action. Using (3) and (4),

$$\overline{AE} = D[\sigma \cdot \dot{\varepsilon} \cdot V_w]^{1/2} \tag{5}$$

where D is a proportionality constant.

Comparing Equations (2) and (5) directly relates AE energy to typical polishing parameters, such as normal pressure, velocity, and abrasive size. In addition, AE signals can be used to describe the surface conditions during polishing because the surface roughness Ra is directly related to the MRR [26], [27], which both shows the polishing efficiency (productivity) and reflects the process/material characteristics.

For the AE signals sampled during material processing, the AE energy is lower for a fracture-dominated region (brittle fracture) than for a plastic flow–dominated area (ductile fracture) [28]. In terms of frequency, low-frequency AE signals are usually generated while processing brittle materials such as IZO, whereas high-frequency signals indicate plastic flow/ductile fracture materials, such as Pyrex glass [20].

III. PROCESS ANALYSIS USING DESIGN OF EXPERIMENTS

A. EXPERIMENTAL SETUP

In this research, a permanent magnet (neodymium) and a direction control piece were added underneath the existing MAF setup to strengthen the magnetic field and control the working areas for effective implementation of nanoscale polishing of micro/nano structures and surfaces inside the selected areas (Fig. 4). The size of the magnet is about the same as the quill (5mm in diameter).

Fig. 4 also illustrates the AE sensor feedback setup for the polishing experiments. A PAC UT1000 broadband sensor was used. AE signals (sampling rate of 2 MHz) were amplified using a pre-amplifier (PAC-1220) and were then sampled using a high throughput data acquisition board (PAC-AEDSP-32). The signals were processed using various signal processing techniques, including AE rms and FFT.

Fig. 5 shows the surface roughness profile of an IZO-coated Pyrex glass workpiece following preliminary experiments (spindle speed = 400 rpm, abrasive size = 125 μm, gap between the quill and workpiece = 0.5 mm, polishing time = 90 seconds) conducted without an extra magnet in the MAF setup. To examine the surface profiles of the polished specimens, a non-contact type 3D interferometric profiler (Nanoview), which measures the surface of sample with nano-level accuracy (vertical resolution of up to 0.1nm), was used.

As stated in the literature [9], the surface finish near the center of the quill is irregular, and the surface roughness values are much higher compared to outside area. In other words, better finishing results are expected if the target finishing area is at the outer area of the quill. Therefore, a direction control piece (for the permanent magnet beneath the

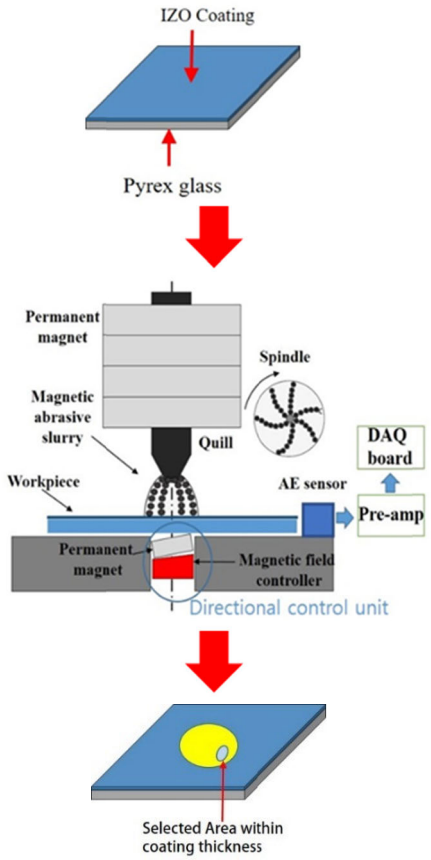

FIGURE 4. Schematic of the proposed setup for the selective finishing of IZO-coated Pyrex glasses using MAF. An extra permanent magnet is placed underneath the MAF setup to strengthen the magnetic field and control the polishing area. A sensor for AE monitoring is also in place.

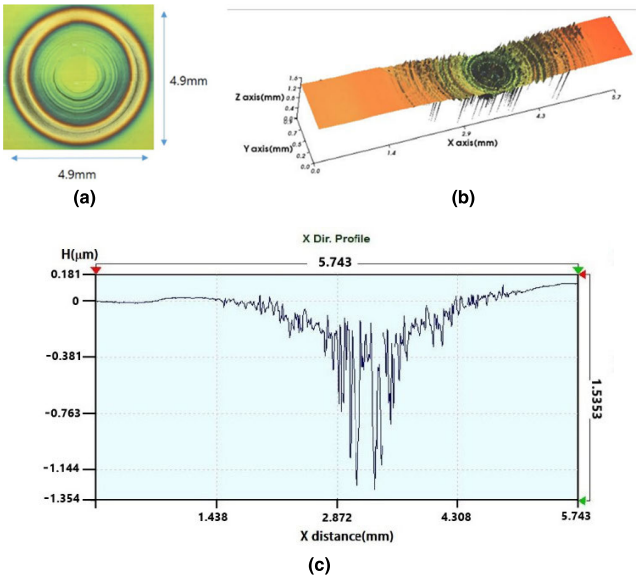

FIGURE 5. The surface profile after MAF (without the underneath magnet setup, spindle speed = 400 rpm, abrasive size = 125 μm, gap between the quill and workpiece = 0.5 mm, polishing time = 90 seconds). As shown in (a), the polished area is about the same size as the quill. In (b) and (c), the irregular surface profile (at the center) are shown. The surface roughness fluctuation range (in (c)) is about 1.5 m over a 5 mm span (x direction).

TABLE 1. Selected parameters and their levels.

Sign	Factor	Unit	Levels		
			1	2	3
A	Spindle Speed	RPM	400	600	800
B	Tool Gap(A)	Mm	0.3	0.4	0.5
C	Magnet Gap(B)	mm	0	1	2
D	Particle Size	μm	25	75	125

workpiece, Fig. 4) was used in the MAF experimental setup to have a uniform and nano level surface finish within a selected area, which is located away from the quill center. With the proposed setup, the reduced polishing area can be selected by tilting the control piece (and the magnet) in a certain direction (say, a specific quadrant direction).

B. DESIGN OF EXPERIMENT AND FINISIHING RESULTS

To evaluate the effects of several parameters (e.g., polishing parameters on the surface roughness) simultaneously, a specially designed experimental process (design of experiment (DOE)) was utilized. After selecting the design parameters and their levels to reflect the effects of experimental conditions on characteristic values [29], an appropriate orthogonal array should be chosen for the experiments.

Appropriate process parameters for optimal surface finishing results were selected from the Preston equation and a related analysis. First, as the normal force is the most influential factor in the polishing process, the gap between the tool and workpiece (Gap A) and the gap between the workpiece and the underneath magnet (Gap B) were chosen as factors. For Gap B, the minimum space for the tilting (1 mm) was not included, and the gap was set at the top center of the magnet. Together with the abrasive size, the RPM was chosen as a factor because it influences the shear force during polishing. After selecting the factors, the levels of each factor were determined in preliminary experiments. The selected factors and their levels (4 factors, 3 levels) are shown in Table 1.

For the DOE, a three-level orthogonal array L_9 (3^4) was chosen. Using the selected parameters and their levels with the proposed double magnet setup, selective finishing experiments were performed three times under each condition in a random order according to the designed table of orthogonal arrays. During the experiments, the AE sensor signals were sampled and processed. At the end of each process run, the surface roughness values (Ra) were measured under each polishing condition (Table 2).

Fig. 6 shows a typical polished area with the direction control piece. The magnet is tilted to the second quadrant direction, so the picture reveals that the polishing action is uniformly concentrated near the center of that quadrant. The

TABLE 2. Designed experiments using orthogonal array (L_9 (3^4)) and results of polishing experiments.

	A	B	C	D	RPM	Gap (A)	Gap (B)	Size	Ave. Ra (nm)
1	1	1	1	1	400	0.3	0	25	86
2	1	2	2	2	400	0.4	1	75	69
3	1	3	3	3	400	0.5	2	125	18
4	2	1	2	3	600	0.3	1	125	74
5	2	2	3	1	600	0.4	2	25	49
6	2	3	1	2	600	0.5	0	75	99
7	3	1	3	2	800	0.3	2	75	74
8	3	2	1	3	800	0.4	0	125	45
9	3	3	2	1	800	0.5	1	25	53

TABLE 3. Optimal process conditions and experimental results.

Symbol		
A	Rotational speed	400 RPM
B	Gap bet. Tool and Glass (Gap A)	0.5 mm
C	Gap bet. Glass and Magnet (Gap B)	2 mm
D	Abrasive size	125 μm
	Average surface roughness (Ra)	18 nm
	Average polishing area	2.1 mm^2

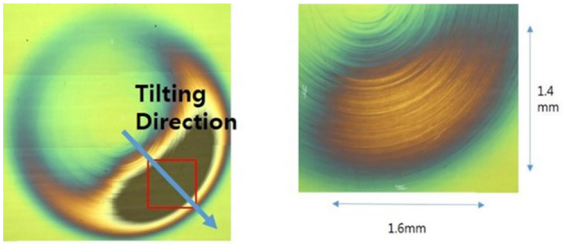

FIGURE 6. Typical polishing results with double magnet setup. With the direction control piece, a reduced polishing area is apparent.

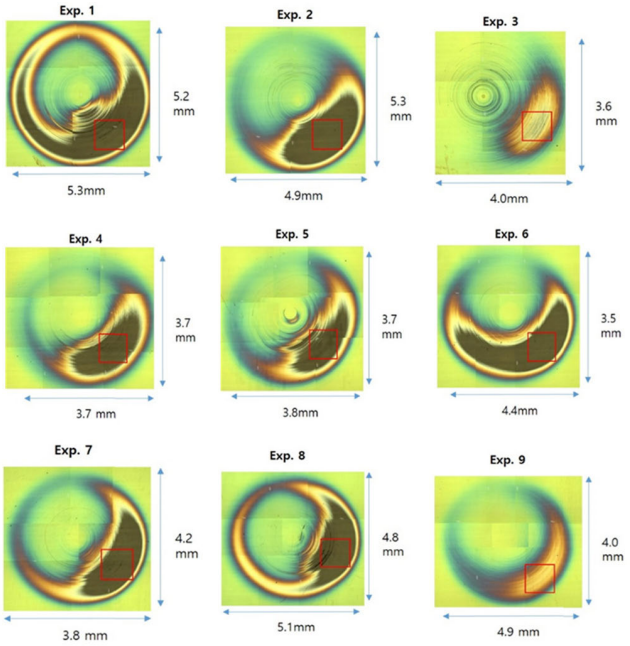

FIGURE 7. Polishing results according to the process conditions by the DOE with the double magnet setup (polishing time = 90sec).

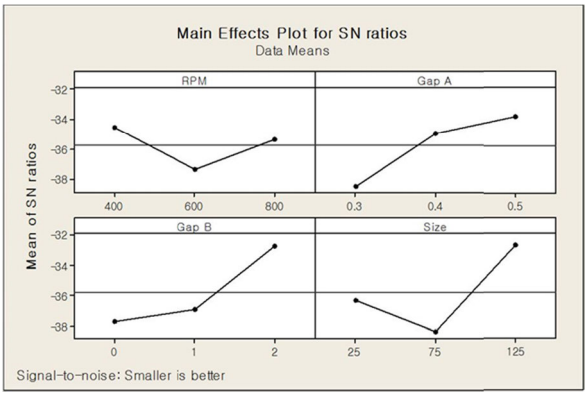

FIGURE 8. Main effects of the parameters on surface roughness with the double magnet setup.

polishing time is 90 seconds, after which most of the IZO coating (200nm in thickness) is removed.

Fig. 7 shows polished workpieces with the double magnet setup using the process conditions from Table 2. Table 3 summarizes the optimal process conditions (those that resulted in the lowest average surface roughness).

Fig. 8 summarizes the influences of the factors on the surface roughness (Ra) as determined by ANOVA (analysis of variance). The figure shows the dispersions and means of levels for each factor with the overall mean value (middle line). As shown in those results, factors B (gap A), C (gap B), and D (abrasive size) were the most influential for surface roughness after polishing.

C. ANALYSIS OF POLISHING RESULTS

1) PARAMETER EFFECTS ON POLISHED SURFACES

Upon analyzing the experimental results, the following effects of each parameter on the polished surface can be summarized. In general, the second magnet underneath the workpiece setup produced some observations distinct from previous MAF results.

1. RPM: As the rotational speed increases, the abrasive particles are more influenced by centrifugal forces, which hinders uniform abrasive polishing of the workpiece surfaces. The optimal rotational speed was 400 rpm.

2. Gap A (between the tool and coated glass workpiece): If the gap is less than a certain value (0.3 mm), the glasses are easily damaged by pressure from the aggregated volume of the magnetic abrasive particles. On the other hand, if the gap is more than 0.5 mm, polishing actions cannot take place because the magnetic field effects are attenuated.

3. Gap B (between the glass and the underneath magnet): If the gap is too close, the magnetic forces of the underneath

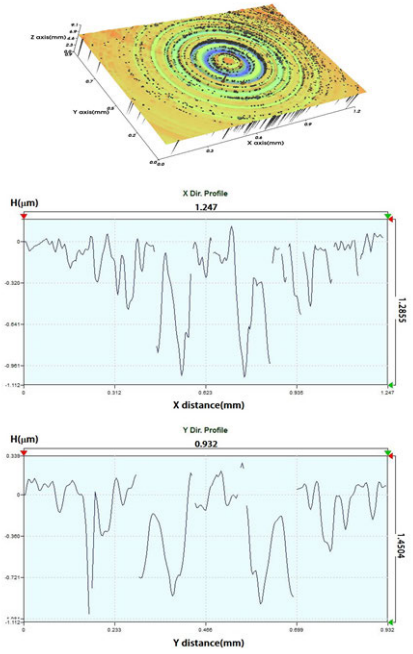

FIGURE 9. The surface topology near the center of the workpiece with the normal MAF setup (no added magnet, 400 RPM, Gap A = 0.5 mm, abrasive size = 125 μm).

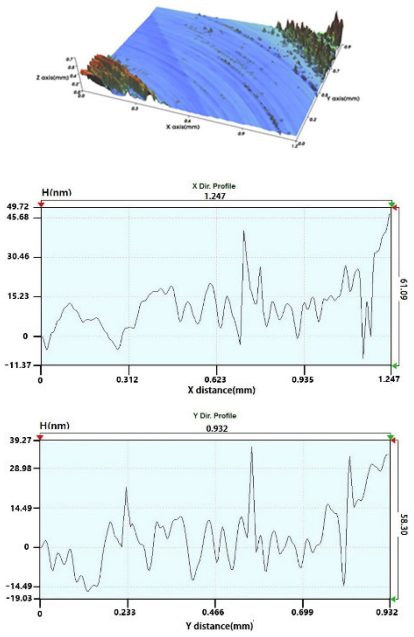

FIGURE 10. The surface topology near the center of the workpiece with the double magnet MAF setup (400 RPM, Gap A = 0.5 mm, abrasive size = 125 μm, Gap B = 2 mm).

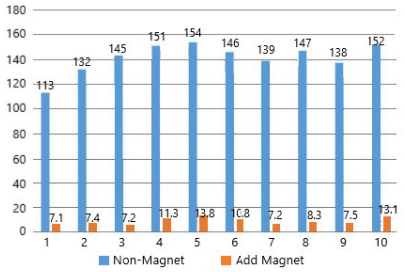

FIGURE 11. Reduced polished area with the double magnet setup.

magnet cause the abrasive particles to stick to the workpiece surface, which results in no polishing action. If the gap is too large (more than 2 mm), the double magnet effects disappear. 4. Size of the magnetic abrasive particles: In normal MAF cases, the surface quality improves (low surface roughness) with smaller abrasives. With the proposed setup, bigger particles (125 μm) showed good surface finishing results. Generating the magnetic fields between the upper magnetic tool and the lower (added) magnet, and using low rpm allows bigger particles to effectively transfer the forces inside the magnetic field.

2) SELECTED AREA FINSIHING RESULTS

To examine the proposed experimental setup, verification/comparison experiments were conducted. With the optimal process conditions given above (400RPM, Gap A = 0.5 mm, abrasive size = 125 μm, Gap B = 2 mm (for the double magnet setup)), polishing tests with and without the underneath magnet were performed.

Fig. 9 shows the surface topology near the center of the workpiece with the normal MAF setup (without magnet). As shown in the figure, the surface roughness fluctuation range is about 1.3 μm over a 1–1.2 mm span. On the other hand, the surface profile with the double magnet setup (Fig. 10) shows much less surface roughness fluctuation (about 50 nm over the same span). In summary, the polishing results with the proposed setup have better and more uniform surface finishing results within the selected working areas (see also Fig. 5).

Fig. 11 compares the polished areas from both MAF setups (with and without the extra magnet). As explained above, the sizes of the magnetic tool and the underneath magnet are both 5 mm. For the without-magnet cases, the polishing areas range 113–154 mm^2 with polishing diameters of 6–7 mm. For the double magnet setup, the polishing areas range 7–13.8 mm^2 with polishing diameters of 1.5–2.1 mm and area reduction ratios of 91–93.8%.

IV. ANALYSIS OF AE MONITORING RESULTS AND ANN

A. AE MONITORING SIGNAL ANALYSIS

For a nano-thickness coating material, detecting the substrate layer during polishing is both important and challenging. Therefore, nanoscale-sensitive AE sensing was adopted to monitor the in-process polishing status. The thickness of the IZO coating is 100nm and 200nm, and with the optimal process conditions given in Table 3, characteristic AE signals at 30, 60, and 90 seconds of polishing time were stored. Then, the processed signals were used in the ANN for process state predictions.

Fig. 12 shows the AE rms (AE energy) variations for different polishing times. Except at the beginning of the process,

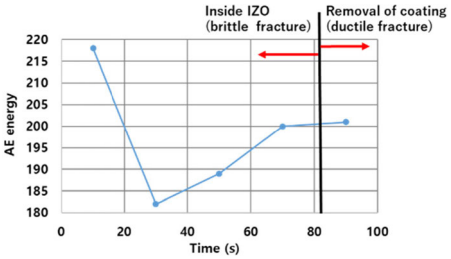

FIGURE 12. AE energy variations as the polishing process progresses.

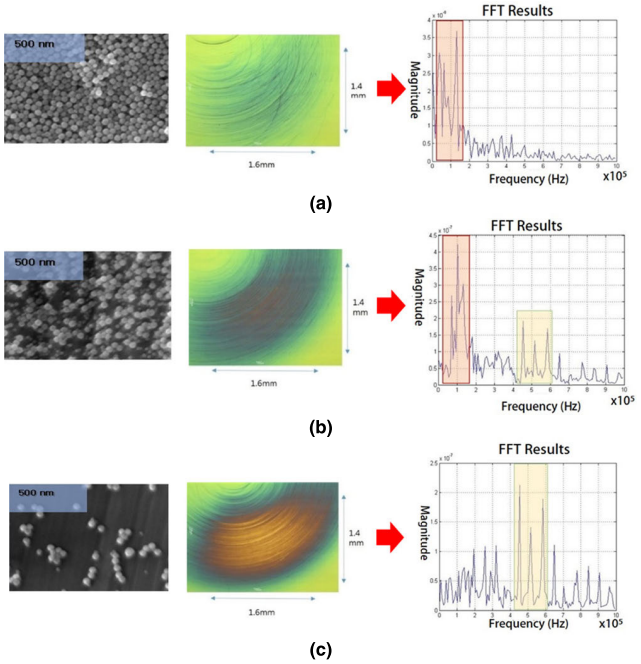

FIGURE 13. Typical surface images and corresponding FFT signals. (a) (rpm = 400, gap A = 0.5 mm, gap B = 2 mm, particle size = 125 μm, polishing time = 30 sec., Ra = 106.7 nm), (b) (rpm = 400, gap A = 0.5 mm, gap B = 2 mm, particle size = 125 μm, polishing time = 60 sec., Ra = 31.7 nm), (C) (rpm = 400, gap A = 0.5 mm, gap B = 2 mm, particle size = 125 μm, polishing time = 90 sec., Ra = 22.9 nm).

the energy levels increase as polishing progresses until the substrate layer (glass) appears, where ductile fractures are likely to occur.

Fig. 13 shows typical images and corresponding AE (frequency) signals during polishing. First, the optical images for different polishing times represent the polishing states of the surfaces. For instance, after just 30s of polishing, scratch marks can be seen on the surface. In addition, an SEM image of the IZO particles at the surface is shown. As the polishing process progresses (60s), the beginning of coating removal can be observed (particles dropping out), followed by the appearance of the glass surface (90s). In terms of AE signals, the average peak frequencies vary from lower values (about 100 kHz at 30s, brittle fracture) to higher values over time. After 60s of polishing, more peaks are observed at the higher frequency range (400–600 kHz, with an average of 150 kHz). After the compete removal of the coating layer (90s), the main peaks are observed mainly in the higher frequency range (average frequency 500 kHz, ductile fracture). The experimental results exhibit the general AE signal characteristics of the materials being processed, as explained above.

TABLE 4. Learning conditions for AE based ANN.

Input Parameters				Targets
IZO Thickness (nm)	Time (sec)	Avg Freq (kHz)	Peak Freq (kHz)	Glass = (1,0) IZO = (0,1)
100	30	96.3	79.8	(0,1)
100	30	94.5	82.6	(0,1)
100	30	98.3	85.2	(0,1)
100	30	96.3	83.2	(0,1)
100	90	408.9	345.9	(1,0)
100	90	418.4	359.6	(1,0)
100	90	423.1	360.4	(1,0)
100	90	421.9	498.7	(1,0)
200	30	114.1	89.7	(0,1)
200	30	115.6	90.1	(0,1)
200	30	112.3	89.4	(0,1)
200	60	212.6	115.4	(0,1)
200	60	204.3	112.3	(0,1)
200	60	216.9	109.9	(0,1)
200	90	515.3	415.6	(1,0)
200	90	512.6	418.7	(1,0)
200	90	514.7	419.1	(1,0)
200	90	509.8	414.9	(1,0)

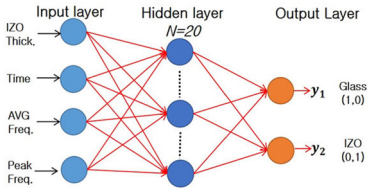

FIGURE 14. Architecture of AE based ANN.

B. BOUNDARY DETECTION USING AE SIGNAL-BASED ANN

An ANN with a back-propagation algorithm, which is frequently used in many practical applications (including ultra-precision, and nanoscale) manufacturing processes [30], [31]), was adopted to detect the coating-substrate boundary.

Back propagation is a supervised learning technique that compares the responses of the output with the desired responses and readjusts the weights in the network so that next time, the network's response to the same input will be closer to the desired output [32]. The learning procedure is very effective because of its simplicity and accuracy [33].

Fig. 14 illustrates the architecture of the ANN with AE-based inputs. The input vectors are composed of processed AE signal data (average AE frequency and peak AE frequency), the IZO coating thickness, and the processing time, which are highly influential parameters for verifying the polishing state. The input values were normalized from 0 to 1 to ensure effective learning and accurate prediction. A total of 27 sets of input data values were selected, and 18

TABLE 5. Input data sets and prediction results with the AE based ANN.

	Input parameters				Targets	Output
Exp No.	IZO (nm)	Time (sec)	Avg Freq (kHz)	Peak Freq (kHz)	Glass=(1,0) IZO=(0,1)	
1	100	30	98.2	81.1	(0,1)	(0.027, 0.889)
2	100	30	97.7	82.6	(0,1)	(0.028, 0.894)
3	100	90	426.3	512.3	(1,0)	(0.903, 0.031)
4	100	90	425.7	511.1	(1,0)	(0.894, 0.036)
5	200	30	109.9	91.2	(0,1)	(0.032, 0.878)
6	200	30	108.7	90.6	(0,1)	(0.033, 0.864)
7	200	30	112.8	91.3	(0,1)	(0.029, 0.894)
8	200	90	516.9	421.2	(1,0)	(0.911, 0.039)
9	200	90	520.1	421.6	(1,0)	(0.891, 0.043)

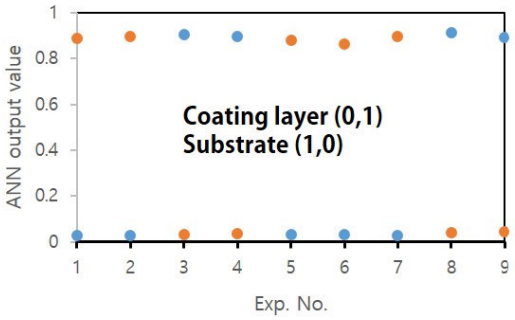

FIGURE 15. Prediction results with AE based ANN.

sets (Table 4) were used for the learning procedure and the rest for the ANN prediction. The target point of the learning process is the time of complete coating removal (90 seconds). After the learning procedures, the input vectors (in Table 5) were fed into the ANN and the predictions were calculated. The processed results are summarized in Table 5 and are plotted against surface conditions (inside the coating and on the substrate) in Fig. 15, which shows that the errors are mostly less than 10%.

V. CONCLUSION

In this research, selective magnetic abrasive finishing of nano-thickness IZO layers on Pyrex substrates were investigated. Optimal process conditions for the nano-order surface finish were acquired, and double magnet setup for a uniform surface finish was implemented in a selected (reduced) area, which is away from the quill center. In addition, an ANN based on AE monitoring signals was constructed to detect the coating-substrate boundary during polishing. The main conclusions are as follows.

(1) By adding a simple permanent magnet unit underneath the existing MAF setup, surface finish and uniformity of an IZO coated glass were upgraded within a target area, leading to selective finishing of micro/nano structures on the coating surface.

(2) Upon analyzing the effects of each parameter on the surface roughness after MAF, the second magnet underneath the workpiece setup produced observations distinct from previous MAF results, especially for the RPM and the abrasive size cases.

(3) AE signals show sensitivity in differentiating the typical polishing states (IZO coating or glass) of nanoscale surface characteristics and detecting the appearance of a ductile substrate (Pyrex glass) as the process progresses. By using features extracted from the AE signals in an ANN, an in-process coating boundary–detection scheme was suggested for nanoscale finishing of a confined area.

(4) Overall, with the proposed double magnet setup and AE monitoring with an artificial intelligence scheme, a comprehensive nano-finishing system with controllable thickness and selective area processing capability became feasible.

REFERENCES

[1] A. P. Malshe, B. S. Park, W. D. Brown, and H. A. Naseem, "A review of techniques for polishing and planarizing chemically vapor-deposited (CVD) diamond films and substrates," *Diamond Rel. Mater.*, vol. 8, no. 7, pp. 1198–1213, Jul. 1999.

[2] X. Li and B. Bhushan, "Micro/nanomechanical and tribological studies of bulk and thin-film materials used in magnetic recording heads," *Thin Solid Films*, vols. 398–399, pp. 313–319, Nov. 2001.

[3] X. Li, B. Bhushan, K. Takashima, C.-W. Baek, and Y.-K. Kim, "Mechanical characterization of micro/nanoscale structures for MEMS/NEMS applications using nanoindentation techniques," *Ultramicroscopy*, vol. 97, nos. 1–4, pp. 481–494, Oct./Nov. 2003.

[4] H.-C. Cheng and C. Y. Tsay, "Flexible a-IZO thin film transistors fabricated by solution processes," *J. Alloys Compounds*, vol. 507, no. 1, pp. L1–L3, Sep. 2010.

[5] K. H. Kim, B. S. Kanga, M.-J. Lee, S.-E. Ahn, C. B. Lee, G. Stefanovich, W. X. Xianyu, K.-K. Kim, J. S. Kim, I. K. Yoo, and Y. Park, "Defect-induced degradation of rectification properties of aged Pt/n-$In_xZn_{1-x}O_y$ Schottky diodes," *Appl. Phys. Lett.*, vol. 92, no. 23, May 2008, Art. no. 233507.

[6] X. N. Xie, H. J. Chung, C. H. Sow, and A. T. S. Wee, "Nanoscale materials patterning and engineering by atomic force microscopy nanolithography," *Mater. Sci. Eng., R, Rep.*, vol. 54, nos. 1–2, pp. 1–48, Nov. 2006.

[7] S. H. Lee, "Surface finishing of nanoscratch patterns on coated pyrex glasses using MAF," *Surf. Rev. Lett.*, vol. 24, no. 4, 2017, Art. no. 1750043.

[8] C.-T. Lin, L.-D. Yang, and H.-M. Chow, "Study of magnetic abrasive finishing in free-form surface operations using the Taguchi method," *Int. J. Adv. Manuf. Technol.*, vol. 34, nos. 1–2, pp. 122–130, Aug. 2007.

[9] L.-D. Yang, C.-T. Lin, and H.-M. Chow, "Optimization in MAF operations using Taguchi parameter design for AISI304 stainless steel," *Int. J. Adv. Manuf. Technol.*, vol. 42, nos. 5–6, pp. 595–605, May 2009.

[10] V. K. Jain, V. Kumar, and M. R. Sankar, "Experimental study and empirical modelling of magnetic abrasive finishing on ferromagnetic and non-ferromagnetic materials," *Int. J. Precis. Technol.*, vol. 3, no. 1, pp. 91–104, 2012.

[11] G. B. Madhab, V. K. Jain, and P. M. Dixit, "On simulation of magnetic abrasive finishing process for plane surfaces using FEM," *Int. J. Mach. Machinability Mater.*, to be published. doi: 10.1504/IJMMM.2006.011063.

[12] D. E. Lee, I. Hwang, C. M. O. Valente, J. F. G. Oliveira, and D. A. Dornfeld, "Precision manufacturing process monitoring with acoustic emission," in *Condition Monitoring and Control for Intelligent Manufacturing*. London, U.K.: Springer, 2006, pp. 33–54.

[13] P. G. Benardos and G. C. Vosniakos, "Predicting surface roughness in machining: A review," *Int. J. Mach. Tools Manuf.*, vol. 43, no. 8, pp. 833–844, Jun. 2003.

[14] Y. Wang, S. Jiang, M. Wang, S. Wang, T. D. Xiao, and P. R. Strutt, "Abrasive wear characteristics of plasma sprayed nanostructured alumina/titania coatings," *Wear*, vol. 237, no. 2, pp. 176–185, Feb. 2000.
[15] T. B. Thoe, D. K. Aspinwall, and M. L. H. Wise, "Review on ultrasonic machining," *Int. J. Mach. Tools Manuf.*, vol. 38, no. 4, pp. 239–255, Mar. 1998.
[16] S. Feygin, G. Kremen, and L. Igelshteyn, "Magnetic-abrasive powder, and method of producing the same," U.S. Patent 2 327 683 A1, Dec. 8, 1998.
[17] G.-W. Chang, B.-H. Yan, and R.-T. Hsu, "Study on cylindrical magnetic abrasive finishing using unbonded magnetic abrasives," *Int. J. Mach. Tools Manuf.*, vol. 42, no. 5, pp. 575–583, Feb. 2000.
[18] F. W. Preston, "The theory and design of plate glass polishing machines," *J. Glass Technol.*, vol. 11, no. 44, pp. 214–256, 1927.
[19] V. H. Bulsara, Y. Ahn, S. Chandrasekar, and T. N. Farris, "Polishing and lapping temperatures," *J. Tribol.*, vol. 119, no. 1, pp. 163–170, Jan. 1997.
[20] B. W. Ahn and S. H. Lee, "Characterization and acoustic emission monitoring of AFM nanomachining," *J. Micromech. Microeng.*, vol. 19, no. 4, Mar. 2009, Art. no. 045028.
[21] S. Koshimizu and J. Otsuka, "Detection of ductile to brittle transition in microindentation and microscratching of single crystal silicon using acoustic emission," *Mach. Sci. Technol.*, vol. 5, no. 1, pp. 101–114, Feb. 2007.
[22] X. Chen, J. Tang, and D. A. Dornfeld, "Monitoring and analysis of ultraprecision metal cutting with acoustic emission," in *Proc. Mech. Eng. Congr. Expo. ASME*, Atlanta, GA, USA, Nov. 1996, p. 387.
[23] J. J. B. Liu, "Monitoring the precision machining process: Sensors, signal processing and information analysis," Ph.D. dissertation, Univ. California, Berkeley, Berkeley, CA, USA, 1991.
[24] R. Hill, *The Mathematical Theory of Plasticity*, vol. 11. London, U.K.: Oxford Univ. Press, 1998.
[25] Y. P. Chang, M. Hashimura, and D. A. Dornfeld, "An investigation of the AE signals in the lapping process," *CIRP Ann.*, vol. 45, no. 1, pp. 331–334, 1996.
[26] R. K. Jain, V. K. Jain, and P. K. Kalra, "Modelling of abrasive flow machining process: A neural network approach," *Wear*, vol. 231, no. 2, pp. 242–248, Jul. 1999.
[27] J. Luo and D. A. Dornfeld, "Material removal mechanism in chemical mechanical polishing: Theory and modeling," *IEEE Trans. Semicond. Manuf.*, vol. 14, no. 2, pp. 112–133, May 2001. doi: 10.1109/66.920723.
[28] T. G. Bifano and Y. Yi, "Acoustic emission as an indicator of material-removal regime in glass micro-machining," *Precis. Eng.*, vol. 14, no. 4, pp. 219–228, Oct. 1992.
[29] G. Taguchi and Y. Yokoyama, *Taguchi Methods: Design of Experiments*, vol. 4. Franklin, MI, USA: American Supplier Institute, 1993.
[30] J. H. Oh and S. H. Lee, "Prediction of surface roughness in magnetic abrasive finishing using acoustic emission and force sensor data fusion," *Proc. Inst. Mech. Eng., B, J. Eng. Manuf.*, vol. 225, no. 6, pp. 853–865, Jul. 2011.
[31] Y.-Y. Lin, S.-P. Lo, S.-L. Lin, and J.-T. Chiu, "A hybrid model combining simulation and optimization in chemical mechanical polishing process," *J. Mater. Process. Technol.*, vol. 202, nos. 1–3, pp. 156–164, Jun. 2008.
[32] Z. Matthew, *Neural Network Models in Artificial Intelligence*. New York, NY, USA: E. Horwood, 1990.
[33] Y. Chauvin and D. Rumelhart, *Backpropagation: Theory, Architectures, and Applications*. Hillsdale, NJ, USA: Lawrence Erlbaum Associates, 1995.

JUNGSUN KIM received the B.S. degree in computer engineering from Seoul National University, South Korea, in 1986, and the M.S. and Ph.D. degrees in electrical engineering and computer engineering from Iowa State University, Ames, IA, USA, in 1988 and 1994, respectively. In 1994, he was a Senior Researcher with the Electronics and Telecommunications Research Institute (ETRI), South Korea. In 1996, he joined the Faculty of the Department of Computer Science and Engineering, Hanyang University, where he is currently a Professor. His current research interests include software architecture, functional programming, and parallel/distributed processing.

HYOJEONG KIM was born in Cheongju, Chungcheongbuk-do, South Korea, in 1994. She received the B.S. degree in mechanical engineering from the University of Korea Polytechnic, Ansan, South Korea, in 2017, and the M.S. degree in mechanical design engineering from Hanyang University, Seoul, South Korea, in 2019, where she is currently pursuing the Ph.D. degree with the Department of Mechanical Design Engineering. Her current research interests include precision machining processes, including magnetic abrasive polishing and manufacturing process monitoring system using acoustic emission.

SEOUNG HWAN LEE received the B.S. and M.S. degrees from Seoul National University, South Korea, and the Ph.D. degree in mechanical engineering from the University of California, Berkeley, Berkeley, CA, USA, in 1996. He is currently a Professor with the Department of Mechanical Engineering with Hanyang University, South Korea. His research interests include the characterization of precision manufacturing including nano scale machining, with special emphasis on precision sensor monitoring and artificial intelligence.